IOPscience iopscience.iop.org

Home Search Collections Journals About Contact us My IOPscience

Double MITs and magnetoresistance: an intrinsic feature of Ru substituted $La_{0.67}Ca_{0.33}MnO_3$

This article has been downloaded from IOPscience. Please scroll down to see the full text article.

2006 J. Phys.: Condens. Matter 18 4427

(http://iopscience.iop.org/0953-8984/18/17/028)

View the table of contents for this issue, or go to the journal homepage for more

Download details:
IP Address: 129.252.86.83
The article was downloaded on 28/05/2010 at 10:25

Please note that terms and conditions apply.

INSTITUTE OF PHYSICS PUBLISHING JOURNAL OF PHYSICS: CONDENSED MATTER

J. Phys.: Condens. Matter **18** (2006) 4427–4442 doi:10.1088/0953-8984/18/17/028

Double MITs and magnetoresistance: an intrinsic feature of Ru substituted $La_{0.67}Ca_{0.33}MnO_3$

L Seetha Lakshmi[1,3], V Sridharan[1], A A Sukumar[2], M Kamruddin[1], V S Sastry[1] and V S Raju[2]

[1] Materials Science Division, Indira Gandhi Centre for Atomic Research, Kalpakkam, Tamil Nadu 603 102, India
[2] National Centre for Compositional Characterization of Materials, Hyderabad, Andra Pradesh-500 062, India

E-mail: slaxmi73@gmail.com

Received 3 January 2006
Published 13 April 2006
Online at stacks.iop.org/JPhysCM/18/4427

Abstract

In this paper, we examine the possible influence of extrinsic factors on the electrical and magnetotransport of $La_{0.67}Ca_{0.33}Mn_{1-x}Ru_xO_3$ ($x \leqslant 0.10$). Ru substitution results in double metal–insulator transitions (MITs) at T_{MI1} and T_{MI2}, both exhibiting magnetoresistance (MR). No additional magnetic signal corresponding to a second low-temperature maximum (LTM) at T_{MI2} could be observed, either in ac susceptibility (χ') or in specific heat (C_p). Typical grain sizes of ∼18 000–20 000 nm, as estimated from the scanning electron microscope (SEM) micrographs, are not so small as to warrant an LTM. The absence of additional peaks in the high statistics powder x-ray diffraction (XRD), a linear systematic increase of the unit cell parameters, close matching of the transition temperatures in resistivity, χ' and C_p and their linear systematic decrease with x, and an homogeneous distribution of Mn, Ru and O at arbitrarily selected regions within and across the grains exclude chemical inhomogeneity in the samples. The insensitivity of grain boundary MR at 5 K to Ru composition indicates that the grain boundary is not altered to result in an LTM. Oxygen stoichiometry of all the compounds is close to the nominal value of 3. These results not only exclude the extrinsic factors, but also establish that double MITs, both exhibiting MR, are *intrinsic* to Ru substituted $La_{0.67}Ca_{0.33}MnO_3$.

1. Introduction

The last decade has seen a renaissance of research activities focused towards the complex ground state properties of the ortho-perovskite manganites [1–5]. Among the most important aspects unveiled is the presence of intrinsically inhomogeneous states in nano- or mesoscopic

[3] Author to whom any correspondence should be addressed.

length scales, sensitive to the external magnetic field [6]. Theories based on microscopic phase separation [7] soon emerged to provide a realistic starting point to the physics of manganites. The multitude of experimental data [8–10] that has poured out in the recent past has indeed established the mixed-phase tendencies in the manganites, consistent with the theoretical predictions. Though many factors are still unexplored or currently under discussion, it is believed that the phase separation in manganites could result from at least two mechanisms: (i) electronic phase separation, where the competing states have different hole densities and $1/r$ Coulomb effects lead to the co-existence of phases at length scales of nanometers; (ii) disorder-driven phase separation near first-order transitions, with competing states of equal density that leads to large (sub-micron) co-existing clusters. These models propose that the competitive magnetic interactions in the background of disorder effects lead to colossal magnetoresistive effects in manganites [11].

Since the essential degrees of freedom (lattice, spin, charge and orbital) are closely associated with the Mn ion, Mn site substitution studies offer a direct method of manipulating the disorder effects. Moreover, suitable paramagnetic substitutions offer an additional handle to probe the local spin coupling, an unexplored parameter of the rare-earth substitution studies. There are numerous works addressing the importance of Mn site substitutions with paramagnetic ions such as Ni^{2+} [12], Cr^{3+} [13, 14], $Ru^{4+/5+}$ [15, 16], and Rh^{3+} [17] in inducing the colossal magnetoresistance (CMR) in the charge ordered (CO) insulating manganites. In these systems, just a few percent substitution ($\sim$3 at.%) at the Mn site is reported to be sufficient for a collapse of the CO state and the appearance of the ferromagnetic state, while a $\sim$7–27 T field is required to melt the CO antiferromagnetic state and induce the CMR effect [18, 19]. Mn site substitution of $Pr_{0.5}Ca_{0.5}MnO_3$ is found to generate two different classes of materials [20]—spin-glass-like insulators, upon diamagnetic and paramagnetic substitutions, result in metallic ferromagnets exhibiting CMR phenomena. Among the paramagnetic substitutions such as Ni^{2+} [12], Co^{3+} [21], Cr^{3+} [13, 22, 23], Ir^{3+} [24], Rh^{4+} [17], and $Ru^{4+/5+}$ [15, 16], the Ru ion is reported to be most efficient in melting the CO state and inducing the ferromagnetism and metallicity in zero magnetic field [25]. For instance, the metal–insulator transition temperature of an Ru substituted compound is reported to be as high as 240 K, while for others it was found to be typically less than 150 K [20]. Hence, Ru appears to be exceptional among the paramagnetic substitutions, which may provide an insight into the nature of the local spin coupling effect on the transport and magnetic properties of CMR manganites.

In our previous studies on the Ru substituted $La_{0.67}Ca_{0.33}MnO_3$ compound, it was found that Ru substitution results in the least reduction in the transition temperatures [26] compared to other paramagnetic substituents [27–31]. From the lowest reduction in the transition temperatures, it was speculated that the local spin coupling between Ru and neighbouring Mn ions is ferromagnetic, and such a local ferromagnetic coupling partially compensates the deleterious local structural effects [26]. Interestingly, Ru substitution results in two metal–insulator transitions [32] (MITs), both exhibiting peaks in the magnetoresistance [33]. Based on the structural, magnetic and electrical and magnetotransport studies of the Ru substituted system and from the inter-comparison of the earlier works, it was speculated that the double maxima in the magnetotransport are closely associated with the MITs. However, as will be discussed in section 3, the double maxima are also shown to arise from extrinsic factors such as synthesis conditions, chemical inhomogeneity, grain size, grain boundary effects, and oxygen off-stoichiometry. To check these possibilities, we have carried out micro-structural studies: SEM and elemental mapping using energy dispersive x-ray analysis (EDAX), magnetoresistance as a function of applied field at 5 K, and thermogravimetric studies (TGA) and the results will be presented in this paper. These results, as will be

discussed subsequently, exclude the extrinsic factors as being the cause of the second low-temperature maximum in the electrical and magneto-transport. The double maxima in the magnetotransport establish the fact that it is intrinsic to Ru substituted $La_{0.67}Ca_{0.33}MnO_3$. This strongly substantiates our hypothesis that the Ru substituted $La_{0.67}Ca_{0.33}MnO_3$ undergoes *a magnetic phase separation* involving the co-existence of two ferromagnetic–metallic (FM-M) phases in its ground state. Though further microscopic experimental studies are in progress, we argue, based on the current knowledge accumulated on the manganite perovskites, that such a magnetic phase separation, distinctly different from the electronic phase separation, is intrinsic to paramagnetic substituted systems with ferromagnetic–metallic ground state. These results are expected to provide a starting point for further theoretical investigations in this area.

2. Experimental details

Polycrystalline samples of $La_{0.67}Ca_{0.33}Mn_{1-x}Ru_xO_3$ ($x \leqslant 0.10$) were prepared by solid state reaction. The final sintering was carried out in a single batch at 1500 °C for 36 h in flowing oxygen. Sufficient care was taken at different stages of sample preparation to ensure that the preparation history is identical for all samples prepared. The room temperature powder XRD patterns with a step size of 0.05° in the 2θ range 15°–120° were recorded in the Bragg–Brentano para-focussing geometry with Cu Kα radiation using a Stoe diffractometer. A dwell time of 30 s was chosen to achieve adequately high statistics ($\sim 10^5$ counts for 100% peak at $2\theta \sim 32.7°$). The XRD patterns were analyzed with the Rietveld method using the GSAS program [34]. The temperature variation of resistivity in zero field ($\rho(T)$) was measured in the van der Pauw geometry [35]. ac susceptibility measurements were performed on powder samples using a home-built ac susceptometer under an ac probe field of 0.25 Oe and an excitation frequency of 941 Hz. The in-phase component of ac susceptibility (χ') alone is considered for further discussion. The magnetoresistance (MR) in an applied field of 5 T was measured using a standard four-probe technique. A superconducting magnet was employed with the magnetic field direction parallel to the current direction. The field- dependent MR measurements were also carried out at 5 K. Specific heat (C_p) measurements were carried out in the temperature interval 140–300 K using a differential scanning calorimeter (Mettler DSC821^e) calibrated for temperature and caloric scales with Ar purge gas. All compounds used had masses of approximately 40 mg. Sapphire was used as the reference material for C_p evaluation. The sample microstructures were recorded using a scanning electron microscope (Philips XL 30) equipped with a field emission gun at 25 keV. Elemental mappings of Mn, Ru and O were carried out at randomly selected areas within the grains and across the grains using an energy dispersive x-ray analysis attachment with an ultra-thin sapphire window Si (Li) detector with 135 eV resolution at 5.9 keV. The oxygen stoichiometry was estimated by decomposing the compounds at 1350 °C under a reducing atmosphere of Ar–4% H_2 mixture flushed at a controlled flow rate. Approximately 30 mg of the powder sample loaded in the recrystallized alumina crucible was heated from room temperature at a linear programmed rate up to 1350 °C in the reducing atmosphere and kept isothermally at 1350 °C for 40 min. A thermogravimetric analyser (SETARAM, Model: SETSYS 16/18) coupled to a mass spectrometer was employed for these studies. The oxygen content of the starting compound was estimated from the weight loss (ΔW) at the end of the isothermal step, assuming the following reduction reactions:

for undoped compound,

$$La_{0.67}Ca_{0.33}MnO_{3\pm\delta} = 0.335La_2O_3 + 0.33CaO + MnO \pm \delta O_2; \quad (1)$$

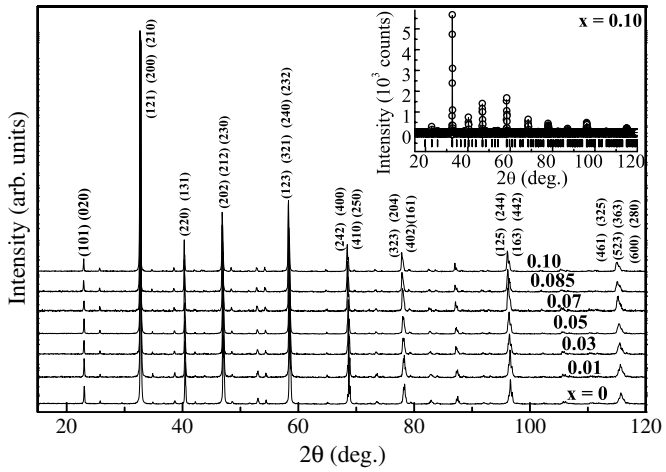

Figure 1. High-statistics room temperature powder x-ray diffraction patterns of $La_{0.67}Ca_{0.33}Mn_{1-x}Ru_xO_3$ ($0 \leqslant x \leqslant 0.10$) compounds. Miller indices of the major Bragg-reflections are also indicated. The inset shows the Rietveld refinement pattern for $x = 0.10$, the highest Ru concentration of the present study. The symbol denotes the observed intensity; continuous lines denote the calculated intensity. The differences between the observed and the calculated intensities are shown at the bottom of the figure. Positions for the calculated Bragg-reflected positions are marked by the vertical bars.

for Ru substituted compounds,

$$La_{0.67}Ca_{0.33}Mn_{1-x}Ru_xO_{3\pm\delta} = 0.335La_2O_3 + 0.33CaO + (1-x)MnO + xRuO_2 \pm \delta O_2. \quad (2)$$

There is close agreement between the percentage weight losses expected for the formation of the final products due to decomposition and those observed in the thermogram. Oxygen off-stoichiometry (δ) was calculated from ΔW according to the relation $\delta = \frac{\Delta W \times W_f}{W_i \times W_O}$, where W_i, W_f and W_O denote the initial weight of the compound, formula weight of the compound, and molecular weight of oxygen, respectively.

3. Results and discussion

High-statistics room temperature powder x-ray diffraction patterns of the compounds are shown in figure 1. All the peaks could be indexed to orthorhombic structure with *Pnma* space group (No. 62). Rietveld refinement yielded excellent agreement between the calculated and the observed patterns, indicating that samples are single phase in nature. As a representative of the series, Rietveld refinement spectra of $x = 0.10$ are shown in the inset of figure 1. It is seen that the lattice parameters a, b and c, and thus cell volume (v), increase linearly with Ru in the entire range of substitution (figure 2). For instance, while a and b show a similar increase of $\sim$0.43% for $x = 0.10$, an increase of $\sim$0.20% is observed for c. The valence state of Ru in these compounds has been a subject of debate [36–38]. Among the possible valence states, the states pertinent to the present study are 3^+, 4^+ and 5^+ with ionic radii of 0.68, 0.62 and 0.565 Å, respectively for six-fold co-ordination [39]. There are reports which propose the presence of Ru^{4+} and Ru^{5+} (iso-electronic to the double exchange pair, Mn^{3+} and Mn^{4+}) ions in these compounds [25, 37]. However, the presence of $Ru^{4+/5+}$ is expected to introduce a decrease in the lattice parameters. On the other hand, the appreciable increase observed in the present case (figure 2) indicates two other possibilities. One such possibility

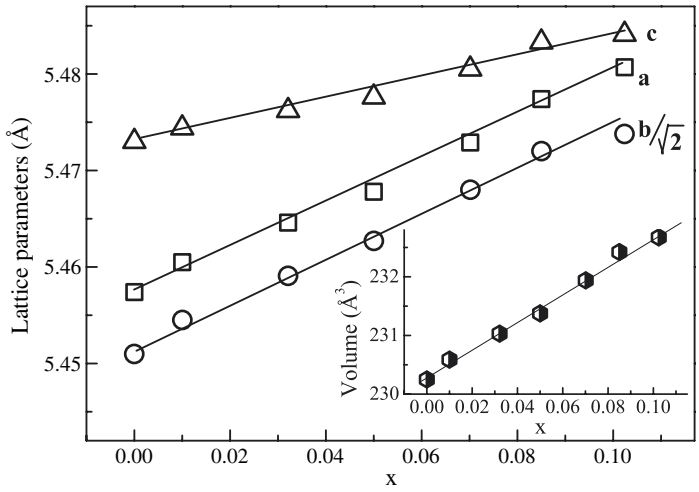

Figure 2. Compositional dependence of lattice parameters (a, b and c) (in Å) and unit cell volume (v) (in Å^3) (inset) of $La_{0.67}Ca_{0.33}Mn_{1-x}Ru_xO_3$ ($0 \leqslant x \leqslant 0.10$) compounds. Error bars are smaller than the symbols. The line is a guide to eye.

is the presence of *either* Ru^{4+} *or* Ru^{3+} with Ru^{4+} replacing Mn^{4+} and Ru^{3+} replacing Mn^{3+} ion. However, inferences from magnetization [32], electrical transport and magnetoresistance measurements, as discussed subsequently, do not favour the presence of Ru^{3+} or Ru^{4+} alone. This strengthens the other possibility of, viz., *Ru being in a mixed valence state of* Ru^{4+} *iso-electronic to* Mn^{3+} *and* Ru^{3+} *being iso-electronic to* Fe^{3+} *ion*, and that such a combination could have led to an increase in the unit cell parameters. X-ray photoemission spectroscopic study on an Ru substituted (La–Sr)–Mn–O system of similar composition [38] has established the presence of Ru^{3+} and Ru^{4+} pairs, and this supports the above inference.

As the temperature is decreased from room temperature, the virgin compound, $La_{0.67}Ca_{0.33}MnO_3$, undergoes a metal-to-insulator transition (MIT), with a sharp maximum at $T = T_{MI}$ in $\rho(T)$ marking a transition from semiconductor-like behaviour ($\partial\rho/\partial T < 0$) to metallic behaviour ($\partial\rho/\partial T > 0$) (figure 3). Close to the MIT, all the compounds exhibit a paramagnetic-to-ferromagnetic transition (PM–FM) at T_c (figure 4). Interestingly, Ru substituted compounds exhibit two maxima in $\rho(T)$: the high-temperature maximum at $T = T_{MI1}$, followed by a relatively broad maximum at still lower temperature ($T = T_{MI2}$) (figure 3). It is worth mentioning that the second low-temperature broad maximum (LTM) is perceptible for $x \geqslant 0.05$. Both the maxima shift systematically to lower temperatures with increasing Ru concentration. While the high-temperature maximum at T_{MI1} shifts at a rate (dT_{MI1}/dx) of ~3 K/at.% up to $x = 0.085$, the smallest rate reported for the Mn site substituted CMR manganites, and much more rapidly beyond that composition, the latter maximum shifts at a rate (dT_{MI2}/dx) ~ 16 K/at.% (figure 5), which is comparable to that of the Fe substituted $La_{0.67}Ca_{0.33}MnO_3$ system [26]. This is in contrast to the charge ordered (CO) Ru substituted $La_{0.4}Ca_{0.6}MnO_3$ [40], where the LTM is reported not to shift with Ru concentration, but remained centred at 125 K. The PM–FM transition associated with T_{MI1} is also found to shift to lower temperatures with $dT_c/dx = 3.2$ K/at.%; no magnetic (ac susceptibility) signal corresponding to a low-temperature maximum could be observed (figure 4). The normalized specific heat curves of $La_{0.67}Ca_{0.33}Mn_{1-x}Ru_xO_3$ ($x \leqslant 0.10$) compounds are given in figure 6. The virgin compound gives rise to a sharp specific heat peak close to its magnetic

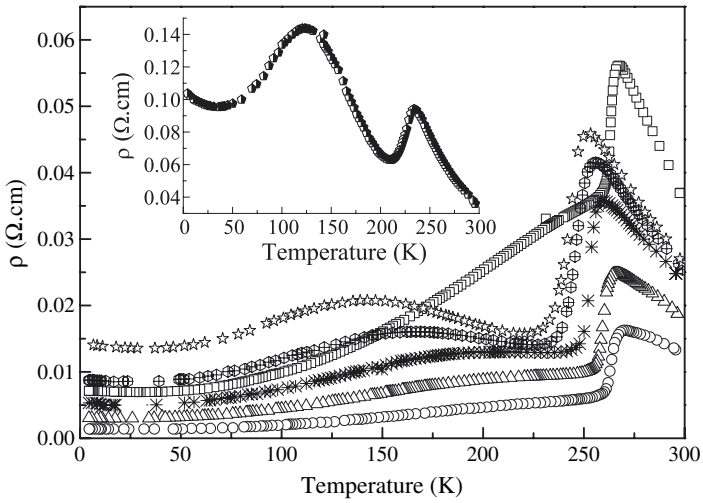

Figure 3. Temperature variation of resistivity ($\rho(T)$) in the absence of magnetic field of $La_{0.67}Ca_{0.33}Mn_{1-x}Ru_xO_3$ compounds for $x = 0$ (□), 0.01 (○), 0.03 (△), 0.05 (✳), 0.07 (⊕), and 0.085 (☆). For clarity, a similar curve for 0.10 (◑) is given in the inset of the figure.

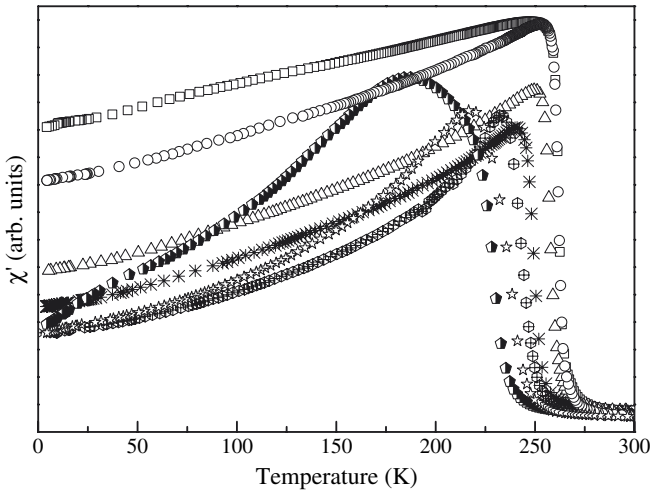

Figure 4. Temperature variation of in-phase component of ac susceptibility ($\chi'(T)$) of $La_{0.67}Ca_{0.33}Mn_{1-x}Ru_xO_3$ compounds (for $x = 0$ (□), 0.01 (○), 0.03 (△), 0.05 (✳), 0.07 (⊕), 0.085 (☆) and 0.10 (◑)) under an ac probe field of 0.25 Oe and an excitation frequency of 941 Hz.

transition (T_c). The specific heat anomaly shifts to lower temperature (the inset of figure 6) and becomes progressively broader with an increase in Ru concentration. These observations are in agreement with that of ac susceptibility measurement. No such anomaly corresponding to T_{MI2} could be observed in our measurements.

With the application of a magnetic field of 5 T, an overall reduction in the resistance was observed (figure 7). As the magnetic field further broadens the inherently broad T_{MI2}, the maximum could not be determined for $x = 0.01$ and 0.03. Though both maxima shift to higher temperature on the application of a magnetic field (a characteristic feature of CMR manganites), their field dependence is somewhat different. While the high-temperature maximum (T_{MI1})

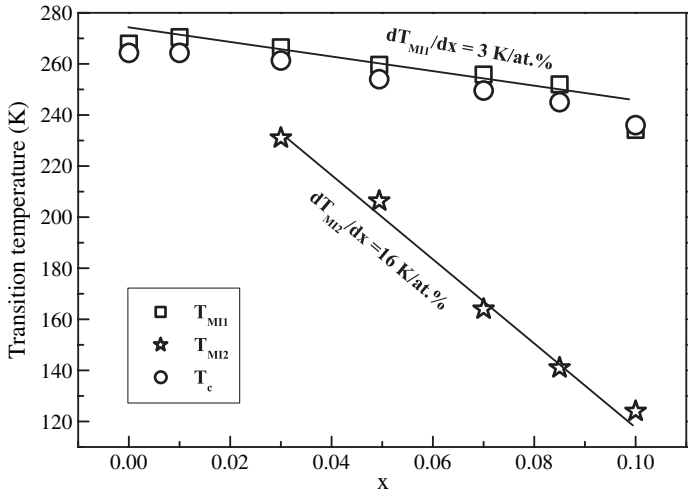

Figure 5. Composition dependence of metal-to-insulator transition temperatures (T_{MI1} and T_{MI2}) and paramagnetic-to-ferromagnetic transition temperature (T_c) of $La_{0.67}Ca_{0.33}Mn_{1-x}Ru_xO_3$ ($0 \leqslant x \leqslant 0.10$) compounds. Straight lines are the best linear fit to the experimental data to estimate the rate of suppression in the transition temperatures.

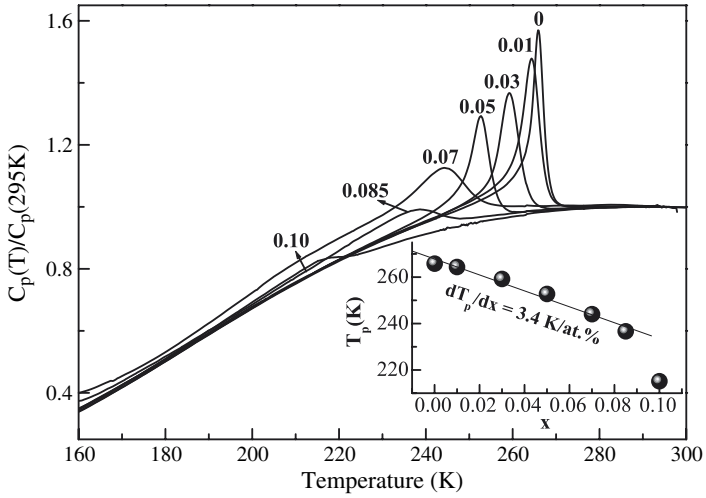

Figure 6. Normalized C_p (curves of $La_{0.67}Ca_{0.33}Mn_{1-x}Ru_xO_3$ ($0 \leqslant x \leqslant 0.10$)) compounds. Inset shows the variation in peak temperature as a function of Ru concentration. Straight line is the best linear fit to the experimental data to estimate the rate of suppression in the transition temperature.

shifts beyond the maximum temperature range of measurement for $x \leqslant 0.07$, the shift of T_{MI2} progressively decreases and a negligible shift is observed for $x = 0.10$. The magnetoresistance (MR), as a percentage, is defined as

$$\mathrm{MR}(\%) = \frac{(\rho_H - \rho_0)}{\rho_0} \times 100 \tag{3}$$

where ρ_H and ρ_0 are the resistivity of the compounds in the presence and absence of magnetic field, respectively. The temperature dependence of MR in a field H of 5 T ($MR_5(T)$) is shown in figure 8. While the MR curve of the undoped compound exhibits a single peak, MR curves

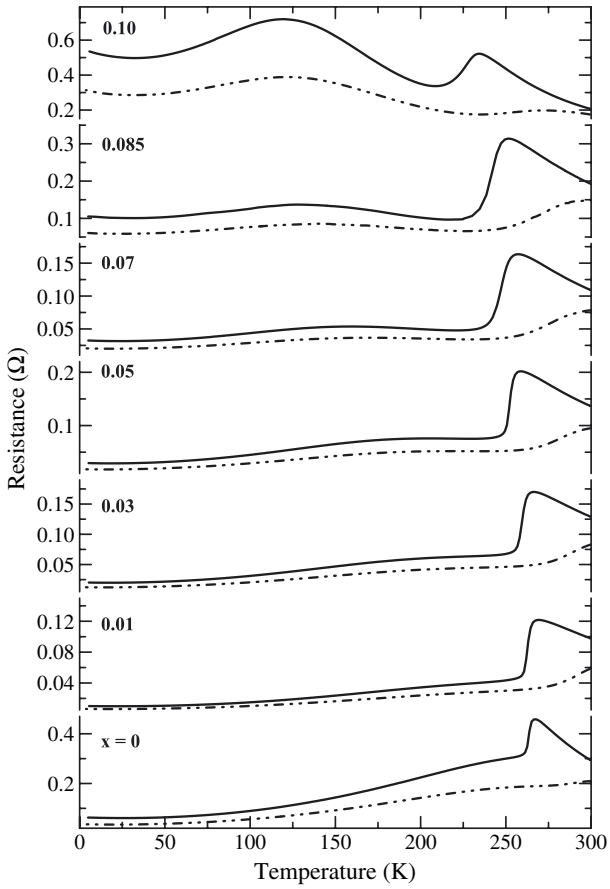

Figure 7. Temperature dependence of resistance in the absence (continuous line) and presence (dotted line) of a magnetic field of 5 T for $La_{0.67}Ca_{0.33}Mn_{1-x}Ru_xO_3$ ($0 \leqslant x \leqslant 0.10$) compounds.

of Ru substituted systems exhibit two peaks: a dominant peak close to its T_{MI1} (in the zero-field resistance) and a weak peak close to its T_{MI2} (in zero-field resistance). Though the latter is arguably weak, it becomes prominent and broader with Ru concentration (figure 8). A significant magnetoresistance with a weak temperature dependence could also be seen well away from the MR peaks, and this is shown to be a characteristic feature of the polycrystalline manganites [41].

Indeed, there are numerous reports on the presence of double maxima in the $\rho(T)$ curve, and most of these reports infer the origin of the double maxima feature to extrinsic factors such as the synthesis conditions [42], chemical inhomogeneity [43, 44], grain size [45, 46], grain boundary (GB) [47, 48], and oxygen off-stoichiometry (δ) [49]. For the present work, it is pertinent to explore if the aforementioned factors are the cause of the LTM of Ru substituted $La_{0.67}Ca_{0.33}MnO_3$. Two maxima in the electrical transport have been observed in ceramics of differently doped La-manganites prepared by sol–gel [45, 50], solid state reactions [51, 52], combustion with urea [53], and the wet chemical method [54]. Of these reports, only the result of Sun *et al* [51] exhibits a sharp and distinct maximum in $\rho(T)$ just near T_c, as observed in Ru substituted compounds. Extreme care was taken at different stages of the synthesis of the compounds for the present investigation. The precursor materials La_2O_3 (Indian-Rare

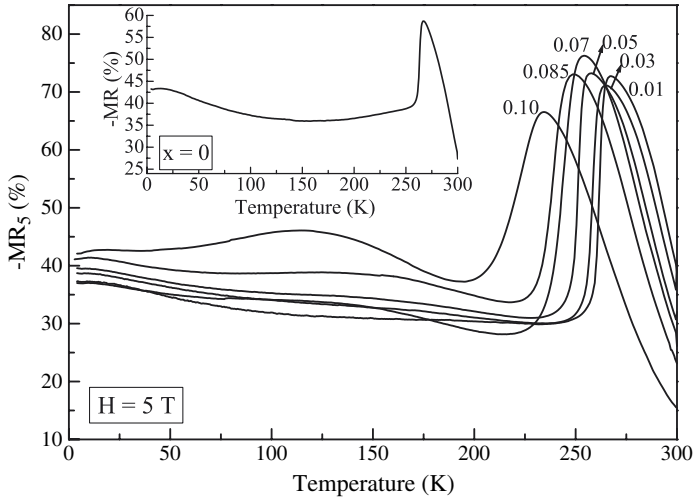

Figure 8. Temperature dependence of magnetoresistance in a 5 T field ($MR_5(T)$) of $La_{0.67}Ca_{0.33}Mn_{1-x}Ru_xO_3$ ($0 \leqslant x \leqslant 0.10$) compounds.

Earths), $CaCO_3$ (*CERAC*), MnO_2 (*CERAC*) and RuO_2 (*CERAC*) are of a purity better than 99.99%. La_2O_3 was pre-heated at 800 °C for 24 h to remove the moisture before weighing. The compounds were given several heat treatments in the temperature range 1200–1400 °C in a flowing oxygen atmosphere with several intermediate grindings followed by pelletization. Sufficient care was taken at different stages so that the preparation history was the same for all samples prepared. The pellets were re-ground and compacted using PVA as a binder to improve the inter-grain connectivity. Added PVA pellets were ramped slowly in the temperature range 200–600 °C and soaked for 3–6 h to remove the traces of PVA. The final sintering at 1500 °C for 36 h in flowing oxygen was carried out in a single batch to ensure that all the samples were given identical sintering conditions. The typical density was determined to be in the range 92–97% of the theoretical value and shows no systematic variation with x. It is believed that the sample synthesis route and the sintering conditions are not the cause for the observed LTM in the Ru substituted compounds of the present study.

Indeed, quite a number of works report LTM in ceramic samples with grain size (GS) less than 1000 nm. For samples with GS of more than 1200 nm, only a single sharp maximum in the $\rho(T)$ curve has been reported. The SEM pictures of the $La_{0.67}Ca_{0.33}Mn_{1-x}Ru_xO_3$ ($x \leqslant 0.10$) compounds are shown in figure 9. It is seen that the GS of the undoped ($x = 0$) compound is ∼20 000 nm. Though the GS marginally decreases with Ru substitution, it is typically in the range 16 000–18 000 nm. An overall improvement in the grain connectivity is observed for the substituted systems. Other studies show that the LTM shifts to lower temperatures with a decrease in GS. For instance, Zhang *et al* [55] have reported a shift of ∼25 K as the GS decreased from 1000 nm to 50 nm and the LTM occurs at ∼250 K for a sample with a GS of 155 nm. In the case of Ru substituted compounds, the LTM shifts at a rate of ∼16 K/at% and it is believed that such a large shift cannot arise from the decrease in GS. For example, the LTM for $x = 0.10$ occurs at ∼120 K. If this is to arise from the GS effect, the GS should be unphysically small [55]. The residual resistivity is shown to increase by a few orders of magnitude with a decrease of GS below 1000 nm. However, the observed increase in ρ_0 in our Ru substituted compounds is far less than this. Another important point to be noted is that $MR(T)$ curves under 5 T show a sharp maximum close to T_{MI1} and a broad maximum close

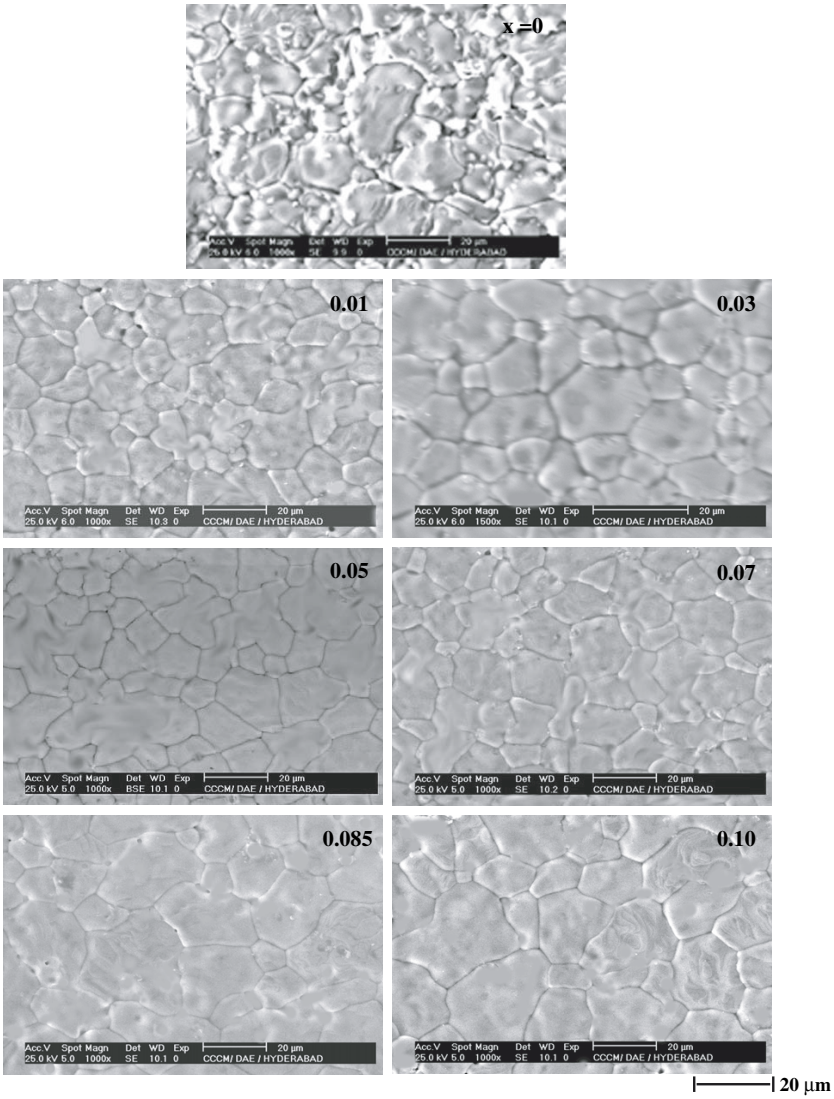

Figure 9. SEM micrograph of $La_{0.67}Ca_{0.33}Mn_{1-x}Ru_xO_3$ ($0 \leqslant x \leqslant 0.10$) compounds.

to T_{MI2} (figure 8). This is in contrast to the reports wherein the latter peak is absent in the MR curve for compounds exhibiting double maxima in the $R(T, H)$ curve due to GS [42, 56]. Additionally, the magnitude of MR at its peak is reported to be sensitive to GS and falls sharply with a decrease in GS. Compounds with smaller GS are shown to exhibit an MR peak value of less than 20% [45], whereas for $x = 0.10$ (the highest Ru concentration of present study) MR peak values as high as 66% and 45% are observed at T_{MI1} and T_{MI2}, respectively (figure 8). The foregoing discussion clearly indicates that GS is certainly not the cause/origin for the observed LTM in the $\mu\rho(T)$ curves of the Ru substituted $La_{0.67}Ca_{0.33}MnO_3$.

The presence of a double maxima feature in the $\rho(T)$ has been reported for the Ln-site substituted $LnMnO_3$ system with Ce^{4+} ion [43, 44]. However, it has been shown that compounds were of a multi-phase nature, evidenced by the presence of additional peak(s)

in the XRD pattern [44]. From the high-statistics XRD pattern collected for Ru substituted compounds, the presence of an impurity phase with a volume fraction of more than 1% is excluded and no peak was left un-indexed (figure 1). The lattice parameters and the unit cell volume are found to increase linearly over the entire range of Ru compositions (figure 2). Additionally, the transition temperatures determined from the resistivity, ac susceptibility (figure 5), and DSC measurements (inset of figure 6) are in close agreement and decrease linearly over the entire composition range, ruling out impurity phase formation. In order to see the chemical homogeneity of the samples, EDAX mapping of Mn, Ru and O is carried out at randomly selected regions within the grain and across the grains. As a representative of the series, the elemental distribution of $La_{0.67}Ca_{0.33}Mn_{1-x}Ru_xO_3$ ($x = 0.085$ and 0.10) compounds are shown in figure 10. The mapping shows a uniform distribution of Mn, Ru and O ions within, as well as across, the grains. This indicates that the compounds are chemically homogeneous within the limitation of the EDAX method. Thus, we rule out chemical inhomogeneity as being the cause of LTM in the $\rho(T)$.

As shown in other works [47, 48, 57], GB can also lead to a broad LTM. The crucial measurement for estimating the GB effects is the evolution of MR under moderate magnetic fields (MR(H)) at different temperatures. The MR versus H curve at 5 K (figure 11) exhibits two slopes: a sharp linear fall for a field less than 1 T, followed by a much slower decrease above 1 T. The GB contribution to MR (GBMR) was estimated by extrapolating high-field MR and finding its intercept at zero field. GBMR for all the compounds at 5 K is found to be ∼24% with systematic variation of Ru concentration (the inset of figure 11). The insensitiveness of GBMR to the Ru composition indicates that GB is not much altered upon Ru substitution to warrant a LTM.

The effect of oxygen off-stoichiometry (δ) in $La_{0.7}Ca_{0.3}MnO_{3-\delta}$ is reported to be as dramatic as any other extrinsic factor mentioned above [49]. Apart from shifting MIT to lower temperatures, it is also reported to result in two maxima in the $\rho(T)$ curves. The width of the transition is reported to be δ dependent, increasing with reducing oxygen content. Larger values of δ are shown to result in a structural transition and render the compound into a semiconductor. Trukhanov *et al* [58] have also shown that, for $\delta > 0.06$, the ferromagnetic–metallic ground state of $La_{0.7}Ca_{0.3}MnO_{3-\delta}$ transforms to a cluster–glass insulator. The TGA curves of $La_{0.67}Ca_{0.33}Mn_{1-x}Ru_xO_3$ ($0 \leqslant x \leqslant 0.10$) compounds are shown in figure 12. The oxygen stoichiometry was found to show a marginal variation from the nominal composition of 3. However, no systematics could be deduced with the Ru composition. If δ is to be the cause of the LTM of the Ru substituted compounds, the expected δ value for $x = 0.10$ is 0.19. On the other hand, the estimated δ for the $x = 0.10$ compound is ∼0.01. Going from the reported works, it is expected that $x \geqslant 0.05$ to undergo a structural transition and to exhibit semiconducting behaviour down to 5 K. However, Ru substituted compounds are found not to alter orthorhombic structure (*Pnma* symmetry) over the entire range of substitution and to retain a metallic ground state. Also, such a large value of δ should have resulted in a drastic increase in the value of ρ_0, typically by a few orders of magnitude. No such large change in ρ_0 is observed in $La_{0.67}Ca_{0.33}Mn_{1-x}Ru_xO_3$ ($0 \leqslant x \leqslant 0.10$) compounds.

From the preceding discussions, it is established that the LTM in the $\rho(T)$ is not due to any of the extrinsic factors. The most striking feature is the presence of a double maximum in the MR(T) curves about their respective metal–insulator transition temperatures. Though the low-temperature MR peak is rather weak for lower x, it becomes dominant and distinct for $x = 0.10$. The LTM in the MR(T) not only *excludes the extrinsic factors* to be the cause of the LTM in the $\rho(T)$, but also establishes the fact that it is *intrinsic* to the $La_{0.67}Ca_{0.33}Mn_{1-x}Ru_xO_3$ system. Having established so, it was proposed for the first time that Ru substituted compounds undergo a magnetic phase separation, different from electronic phase separation occurring in

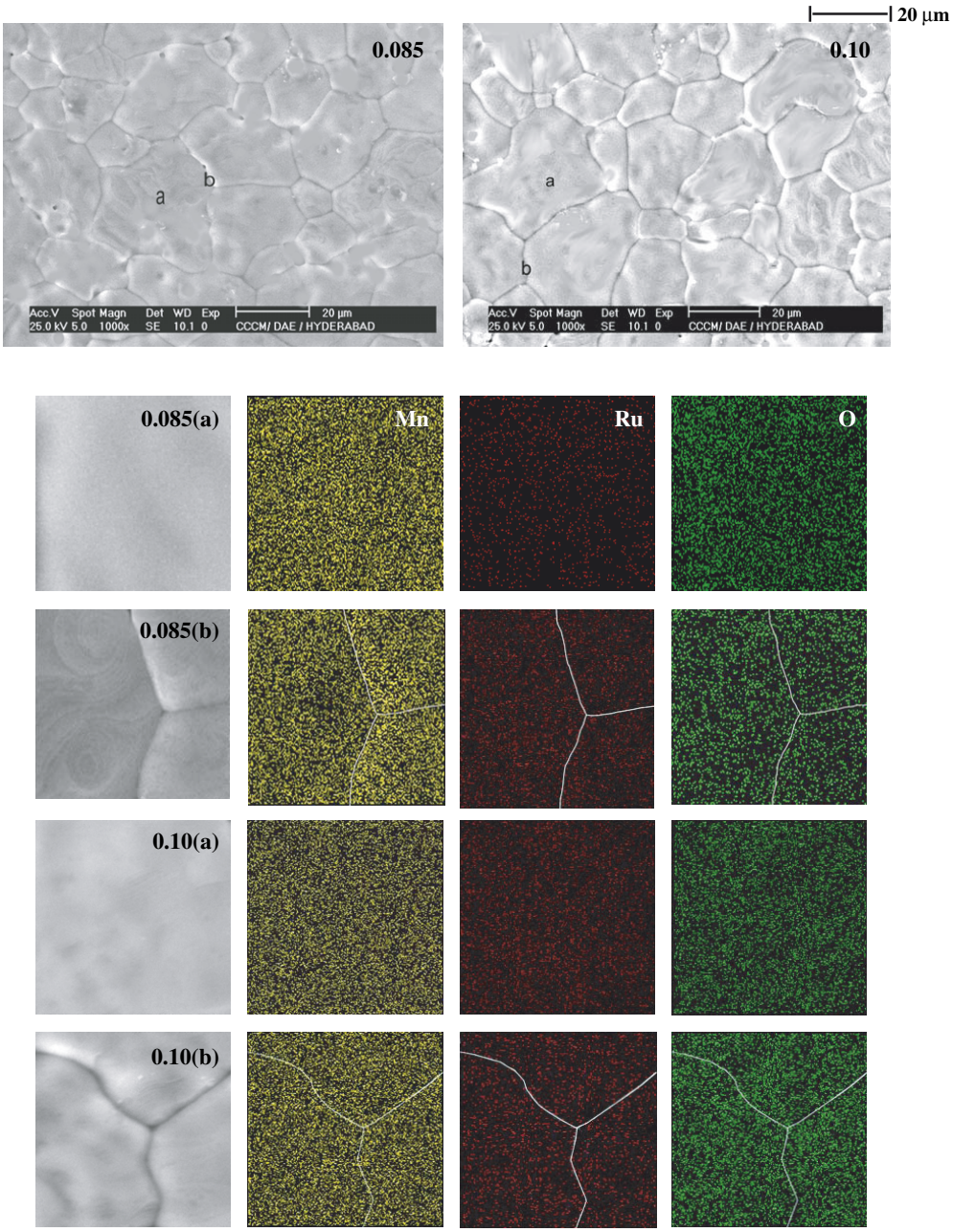

Figure 10. EDAX map of Mn, Ru and O in the selected regions (a) within the grain and (b) across the grains of $La_{0.67}Ca_{0.33}Mn_{1-x}Ru_xO_3$ ($x = 0.085$ and 0.10) compounds. For a comparison, the corresponding SEM micrographs are also shown in the topmost panel.

(This figure is in colour only in the electronic version)

other systems where AFM-I and FM-M transitions coexist at low temperatures [6, 59]. The volume fraction of these two phases in the electronic phase separated system could easily be

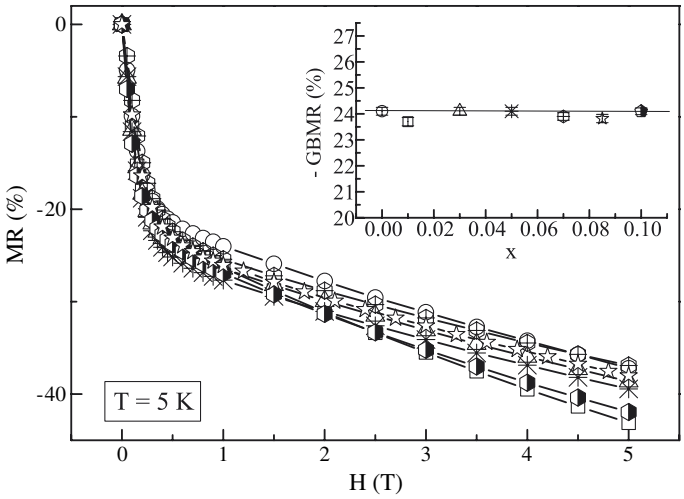

Figure 11. Field dependence of MR (MR(H)) at 5 K of $La_{0.67}Ca_{0.33}Mn_{1-x}Ru_xO_3$ compounds ($x = 0$ (□), 0.01 (○), 0.03 (△), 0.05 (✳), 0.07 (⊕), 0.085 (☆) and 0.10 (◑)). The inset shows the variation of GBMR (in %) at 5 K as a function of the x for the compounds.

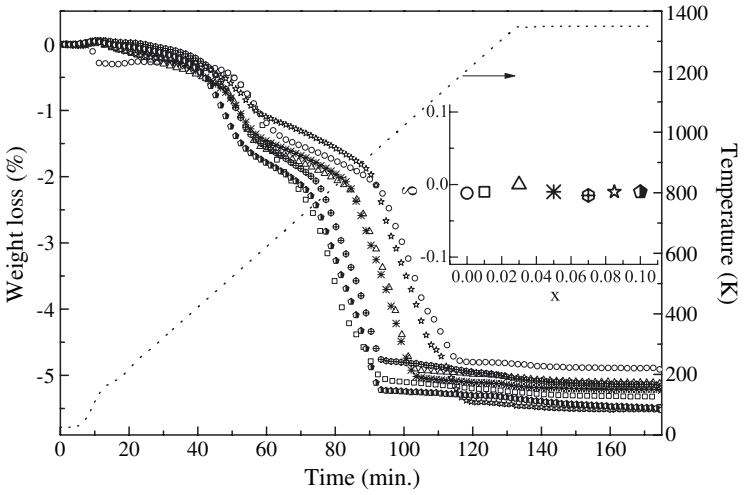

Figure 12. TGA curves of $La_{0.67}Ca_{0.33}Mn_{1-x}Ru_xO_3$ compounds for $x = 0$ (□), 0.01 (○), 0.03 (△), 0.05 (✳), 0.07 (⊕), 0.085 (☆) and 0.10 (◑). The inset shows the oxygen off-stoichiometry (δ) as a function of x for the compounds.

altered by a suitable thermodynamic variable such as magnetic field, pressure or by chemical doping, as in the case of $(La_{1-x}Pr_x)_{0.67}Ca_{0.33}MnO_3$ system [6]. With the increase of the AFM-I phase, i.e. by increasing the Pr concentration, ρ_0 is found to increase by several orders of magnitude. In contrast, in the case of Ru substituted $La_{0.67}Ca_{0.33}MnO_3$ compounds, ρ_0 increases by a factor of five [32]. Also, in the case of *electronic phase separation*, only a single maximum in the resistivity curves is expected since, out of the two phases, the FM phase alone is metallic in nature. Thus it is concluded that the phase separation encountered in Ru substituted $La_{0.67}Ca_{0.33}MnO_3$ compounds is not an electronic phase separation, since both the phases are FM-M in their ground state. Nevertheless, they could still differ in their magnetic

properties. The difference in the electrical transport and magnetic properties, influenced by the strength of double exchange (DE) interaction, can be rationalized in the following way.

Drawing an analogy with the Fe^{3+} substituted $La_{0.67}Ca_{0.33}MnO_3$ compounds having a dT_c/dx of ∼18 K/at% [26], and also in the light of x-ray photoelectron spectroscopy (XPS) studies on the Ru doped La–Sr–Mn–O system by Krishnan *et al* [38] and x-ray magnetic circular dichroism (XMCD) studies by Weigand *et al* [60], the mixed valence state of Ru, viz, Ru^{4+} (iso-electronic to Mn^{3+}) and Ru^{3+} (iso-electronic to Fe^{3+}), has been inferred. The double maxima in the $\rho(T)$ curve correspond to the evolution of two ferromagnetic–metallic phases: Ru^{4+}-rich regions with local ferromagnetic coupling of Ru with the neighbouring Mn ions and Ru^{3+}-rich regions with local antiferromagnetic coupling of Ru with neighbouring Mn ions. Of the two FM phases, the latter is a weaker ferromagnetic phase. The local ferromagnetic coupling between Ru^{4+} and neighbouring Mn spins favours the DE interaction strength, leading to a small dT/dx (∼3 K/at%) associated with T_{MI1}, T_c and $T(C_p)$. On the other hand, a Ru^{3+} ion with its half-filled electronic configuration cannot participate in DE interaction. Moreover, its local AFM coupling with neighbouring Mn spins in the presence of competing aniferromagnetic super-exchange interactions weakens the DE interaction strength, which in turn results in a larger suppression rate (dT_{MI2}/dx) of ∼16 K/at% comparable to that of Fe^{3+} substituted CMR manganites. Progressive lowering of T_{MI1} and T_{MI2} with Ru concentration indicates that the corresponding phases are becoming progressively enriched in Ru^{4+} and Ru^{3+}, respectively. The enrichment of Ru^{3+} and/or an increase in the volume fraction of the weaker ferromagnetic (poor conducting) phase is expected to result in the observed rise in the value of ρ_0 of the substituted compounds. The origin of the double maxima in $\rho(T)$ can then be understood in the context of magnetic phase separation. A more detailed discussion of the magnetic phase separation scenario is published elsewhere [33]. As the sample is cooled down from higher temperatures (i.e. the paramagnetic insulating phase), a ferromagnetic phase (FM-M1) evolves within a paramagnetic (PM) matrix, having appreciable resistivity contrast between the phases. Upon reaching a critical volume fraction V_C, FM-M1 establishes a percolative path and the resistivity drops drastically, resulting in a maximum in $\rho(T)$. On further cooling, the PM phase itself undergoes a paramagnetic-to-ferromagnetic transition. As the system is percolatively conducting below T_{MI1}, the magnetic transition of the PM phase is not expected to produce a drastic drop in the resistivity, as seen for T_{MI1}. The magnetic field results in an expected shift of T_{MI1} to higher temperature. Such a shift is not expected in the case of T_{MI2} for the reason that the magnetic transition of the PM phase takes place within a conducting FM-M1 matrix with a low conductivity contrast. This magnetoresistance signal corresponding to the LTM in zero-field resistivity grows into a broad maximum under a magnetic field of 5 T, but far smaller compared with that of T_{MI1}. These features, a negligible shift of T_{MI2} and a substantially reduced MR maximum associated with T_{MI2}, support the conjecture of a magnetic phase separation occurring in $La_{0.67}Ca_{0.33}Mn_{1-x}Ru_xO_3$ compounds.

4. Conclusions

The possible role of the extrinsic factors such as synthesis conditions, chemical inhomogeneity, grain size, grain boundary effects, and oxygen-off stoichiometry for the second low-temperature maximum on the electrical transport of Ru substituted $La_{0.67}Ca_{0.33}MnO_3$ are analysed in the light of the SEM, EDAX, field-dependent magnetoresistance and thermogravimetric studies. In our opinion, synthesis conditions do not play a role in the electrical transport of the Ru substituted system. Typical grain sizes of ∼18 000–20 000 nm, as estimated from the SEM micrographs, are not so small as to warrant an LTM. The absence of any additional peaks in high-statistics XRD patterns, a linear systematic increase of the unit cell

parameters, close matching of the transition temperatures in the resistivity, ac susceptibility and specific heat, the linear systematic decrease in the transition temperatures with Ru composition, and homogeneous distribution of Mn, Ru and O at arbitrarily selected areas within the grain and across the grains rule out chemical inhomogeneity in the samples. The insensitivity of grain boundary contribution of MR at 5 K to the Ru composition indicates that the grain boundary is not altered much on Ru substitution to warrant an LTM in the electrical transport. The oxygen stoichiometry of the compounds is close to the nominal composition of 3. These results not only exclude the extrinsic factors, but also establish unambiguously that the double metal–insulator transitions, both exhibiting magnetoresistance, are intrinsic to Ru substitution. These results substantiate our hypothesis that the Ru substituted system undergoes a magnetic phase separation involving the co-existence of two ferromagnetic–metallic phases in its ground state.

Acknowledgments

We wish to thank Dr R Rawat of the UGC-CSIR Consortium for Scientific Research, Indore, India for the magnetoresistance studies, Dr T Geethakumary, MSD, IGCAR for providing the ac susceptibility set up, and Mr P K Ajikumar, MSD, IGCAR for the thermogravimetric studies. One of the authors, LSL, also acknowledges the Council of Scientific and Industrial Research, India, for the award of a Senior Research Fellowship.

References

[1] Tokura Y (ed) 2000 *Colossal Magnetoresistive Oxides* (London: Gordon and Breach Science Publishers)
[2] Salamon M B and Jaime M 2001 *Rev. Mod. Phys.* **73** 583
[3] Ziese M 2002 *Rep. Prog. Phys.* **65** 143
[4] Dagotto E 2003 Nanoscale phase separation and colossal magnetoresistance *Springer Series in Solid-State Science* vol 136 (Berlin: Springer)
[5] Dagotto E 2005 *New. J. Phys.* **7** 67
[6] Uehara M, Mori S, Chen C H and Cheong S-W 1999 *Nature* **399** 560
[7] Dagotto E, Hotta T and Moreao A 2001 *Phys. Rep.* **344** 1 and references therein
[8] Fath M, Freisem S, Menovsky A A, Tomioka Y, Aarts J and Mydosh J A 1999 *Science* **285** 1540
[9] Billinge S J L, Proffen Th, Petkov V, Sarrao J L and Kycia S 2000 *Phys. Rev.* B **62** 1203
[10] Heffner R H, Sonier J E, MacLaughlin D E, Nieuwenhuys G J, Ehlers G, Mezei F, Cheong S-W, Gardner J S and Röder H 2000 *Phys. Rev. Lett.* **85** 3285
[11] Burgy J, Mayr M, Martin-Mayor V, Moreo A and Dagotto E 2001 *Phys. Rev. Lett.* **87** 277202
[12] Maignan A, Damay F, Martin C and Raveau B 1997 *Mater. Res. Bull.* **32** 965
[13] Damay F, Martin C, Maignan A, Hervieu M, Bourée F and André G 1999 *Appl. Phys. Lett.* **73** 3772
[14] Raveau B, Martin C and Maignan A 1998 *J. Alloys Compounds* **275–277** 461
[15] Martin C, Maignan A, Hervieu M, Autret C and Raveau B 2001 *Phys. Rev.* B **63** 174402
[16] Raveau B, Martin C, Maignan A, Hervieu M and Mahendiran R 2000 *Physica* C **341–348** 711
[17] Raveau B, Hérbert S, Maignan A, Frésard R, Hervieu M and Khomski D 2001 *J. Appl. Phys.* **90** 1297
[18] Tomioka Y, Asamitsu A, Kuwahara H, Moritomo Y and Tokura Y 1996 *Phys. Rev.* B **53** R1685
[19] Tokunaga M, Miura N, Tomioka Y and Tokura Y 1998 *Phys. Rev.* B **57** 5259
[20] Hébert S, Maignan A, Martin C and Raveau B 2002 *Solid State Commun.* **121** 229
[21] Raveau B, Maignan A and Martin C 1997 *J. Solid State Chem.* **130** 162
[22] Martin C, Maignan A, Damay F, Hervieu M, Raveau B, Jirak Z, André G and Bourée F 1999 *J. Magn. Magn. Mater.* **202** 11
[23] Mahendiran R, Hervieu M, Maignan A, Martin C and Raveau B 2000 *Solid State Commun.* **114** 429
[24] Hébert S, Maignan A, Frésard R, Hervieu M, Retoux R, Martin C and Raveau B 2001 *Eur. Phys. J.* B **24** 85
[25] Maignan A, Martin C, Hervieu M and Raveau B 2001 *J. Appl. Phys.* **89** 500
[26] Seetha Lakshmi L, Sridharan V, Natarajan D V, Sastry V S and Radhakrishnan T S 2002 *Pramana-J. Phys.* **58** 1019
[27] Rao G H, Sun J R, Kattwinkel A, Haupt L, Bärner K, Schmitt E and Gmelin E 1999 *Physica* B **269** 379
[28] Sun Y, Xu X and Zhang Y 2001 *Phys. Rev.* B **63** 054404

[29] Rivadulla F, López-Quintela M A, Hueso L E, Sande P and Rivas J 2000 *Phys. Rev.* B **62** 5678
[30] Yuan L, Zhu Y and Ong P P 2001 *Solid State Commun.* **120** 495
[31] Gayathri N, Raychaudhuri A K, Tiwary S K, Gundakaram R, Arulraj A and Rao C N R 1997 *Phys. Rev.* B **56** 1345
[32] Seetha Lakshmi L, Sridharan V, Natarajan D V, Chandra S, Sastry V S, Radhakrishnan T S, Pandian P, Joseyphus R J and Narayanasamy A 2003 *J. Magn. Magn. Mater.* **257** 195
[33] Seetha Lakshmi L, Sridharan V, Natarajan D V, Rawat R, Chandra S, Sastry V S and Radhakrishnan T S 2004 *J. Magn. Magn. Mater.* **279** 41
[34] Larson A C and von Dreele R B 2000 *Los Alamos National Laboratory Report* LAUR pp 86–748
[35] van der Pauw 1958 *Philips Res. Rep.* **13** 1
[36] Kim J S, Kim B H, Kim D C, Lee H J, Kim M G, Maignan A, Raveau B and Park Y W 2004 *J. Superconductivity: Incorporating Novel Magnetism* **17** 183
[37] Sahu R K and Manoharan S S 2000 *Appl. Phys. Lett.* **77** 2382
[38] Krishnan K M and Ju H L 1999 *Phys. Rev.* B **60** 14793
[39] Shannon R D and Prewitt C T 1976 *Acta Crystallogr.* A **32** 751
[40] Raveau B, Maignan A, Martin C, Mahindran R and Hervieu M 2000 *J. Solid State Chem.* **151** 330
[41] Hwang H Y, Cheong S-W, Ong N P and Batalogg B 1996 *Phys. Rev. Lett.* **77** 2041
[42] Zhang L W, Chen Z J, Di L F, Cao B S, Zhu M H and Zhao Y G 2000 *Phys. Status Solidi* a **179** 205
[43] Gebhardt J R, Roy S and Ali N 1999 *J. Appl. Phys.* **85** 5390
[44] Mitra C, Raychaudhuri P, John J, Dhar S K, Nigam A K and Pinto R 2001 *J. Appl. Phys.* **89** 524
[45] Zhang N, Wang F, Zhong W and Ding W 1999 *J. Phys.: Condens. Matter* **11** 2625
[46] Shiyaktin O A, Oh Y-J and Tretyakov Y D 1999 *Solid State Commun.* **111** 711
[47] Vertruyen B, Cloots R, Rulmont A, Dhalenne G, Ausloos M and Vanderbrmden Ph 2001 *J. Appl. Phys.* **90** 5692
[48] Klein J, Höfener C, Uhlenbruck S, Alff L, Büchner B and Gross R 1999 *Europhys. Lett.* **47** 371
[49] Malavasi L, Mozzati M C, Azzoni C B, Chiodelli G and Flor G 2002 *Solid State Commun.* **123** 321
[50] Zhang N, Ding W, Zhong W, Xing D and Du Y 1997 *Phys. Rev.* B **56** 8138
[51] Sun J R, Rao G H and Zhang Y Z 1998 *Appl. Phys. Lett.* **72** 3208
[52] Mandal P and Das S 1997 *Phys. Rev.* B **56** 15073
[53] Vertruyen B, Rulmont A, Cloots R, Ausloos M, Dorbolo S and Vanderbemden P 2002 *Mater. Lett.* **57** 598
[54] Philip J and Kutty T R N 2001 *Appl. Phys. Lett.* **79** 209
[55] Zhang N, Zhang S, Ding W, Xing D and Du Y 1998 *Chin. J. Phys.* **36** 128
[56] Zhang N, Ding W and Zhong W 1999 *Phys. Lett.* A **253** 113
[57] Gross R, Alff L, Büchner B, Freitag B H, Höfener C, Klein J, Lu Y, Mader W, Philipp J B, Rao M S R, Reutler P, Ritter S, Thienhaus S, Uhlenbruck S and Wiedenhorst B 2000 *J. Magn. Magn. Mater.* **211** 150
[58] Trukhanov S V, Kasper N V, Troyanchuck I O, Tovar M, Szymczak H and Bärner K 2002 *J. Solid State Chem.* **169** 85
[59] Machida A, Moritomo Y, Ohoyama K, Katsufuji T and Nakamura A 2002 *Phys. Rev.* B **65** 064435
[60] Weigand F, Gold S, Schmid A, Geissler J, Goering E, Dörr K, Krabbes G and Ruck R 2002 *Appl. Phys. Lett.* **81** 2035